A high-precision and fast 3D CSEM forward method for the multi-scale hydraulic fracturing model considering anisotropy and micro-fracture structures

Zhitao XIONG, Xingong TANG*
Key Laboratory of Exploration Technologies for Oil and Gas Resources of MOE, Yangtze University, Wuhan 430100, China

SUMMARY

In the forward calculation of multi-scale hydrofracturing geo-electrical models, efficiency and accuracy when handling very thin hydraulic fractures is still a big challenge. The quantitative interpretation of electromagnetic monitoring data for hydraulic fracturing involves multi-scale simulations of millimeter-scale fractures within kilometer-scale background formations. This requires designing complex grids and solving large Maxwell equations, leading to low computational efficiency. This paper employs effective medium theory to establish the relationship between the microscopic geometric parameters of hydraulic fractures and the macroscopic anisotropic conductivity of the fractured formation. In the forward modeling, the effective anisotropic medium, which can describe the microscopic geometric structure of fractures, is used to replace the fracture medium in the hydraulic fracturing section. This approach achieves efficient forward modeling of controlled-source electromagnetic methods for multi-scale hydraulic fracturing models that consider the microscopic geometric structure of fractures. Model calculations reveal that even under the same transformation volume and fracturing fluid content, the deflection of hydraulic fractures significantly affects the anomalous distribution of the surface monitoring electric field. This study indicates that in the interpretation of fracturing electromagnetic monitoring data, besides the known significant steel casing effect, the anisotropy of the fractured formation is another crucial factor that needs to be considered.

Keywords: CSEM；Effective medium theory；Anisotropy；Hydraulic fracturing

INTRODUCTION

Hydraulic fracturing technology is essential for developing shale gas, as it modifies the tight shale reservoirs. The extent of hydraulic fracture development and its microscopic structure in the modified reservoir are key parameters for evaluating the effectiveness of fracturing development and estimating shale gas productivity. However, accurately obtaining the geometric parameters of hydraulic fractures remains a challenging issue for both academia and industry (Li et al., 2023).

In the forward calculations of multi-scale hydraulic fracturing geoelectric models, handling slender steel casings and extremely thin hydraulic fractures leads to low computational efficiency and precision in existing forward algorithms. Various algorithms have been proposed for simulating steel casings, but relatively few studies have focused on the electromagnetic effects of hydraulic fractures. Currently, thin plates are often used to approximate the macroscopic effects of fractures in fracturing sections (Weiss et al., 2016; Hoversten and Schwarzbach, 2021). This method has limited ability to improve the speed of forward calculations and cannot quantitatively consider the microscopic structure of complex fracture networks. Berryman and Hoversten (2013) studied the relationship between fracture parameters and effective conductivity using a self-consistent effective medium theory. However, their results are limited when applied to the extreme aspect ratios of hydraulic fractures in shale gas development.

This paper uses effective medium theory to study the relationship between the geometric parameters of hydraulic fractures and anisotropic conductivity. In the forward calculations, an anisotropic medium that can describe the microscopic structure of fractures replaces the fracture medium in the hydraulic fracturing section. This approach not only significantly reduces the number of grid subdivisions in the model, greatly improving the efficiency of forward calculations, but also establishes a bridge between the geometric parameters of hydraulic fractures and the macroscopic electromagnetic response. This lays the foundation for accurately inverting the

geometric parameters of hydraulic fractures and refining the interpretation of time-lapse electromagnetic monitoring data.

METHOD

Fractures are approximated as extremely thin ellipsoids. Only the conductivity of the background medium and fracturing fluid are considered. The effective conductivity of the fracture medium, constructed using effective medium theory, is expressed as (Berryman and Hoversten, 2013),

$$\sum_{i=0}^{3} \phi_i \left(\boldsymbol{\sigma} - \sigma_i \boldsymbol{I}\right) \bullet \boldsymbol{R}^{(i,0)} = 0 \qquad (1)$$

where i=0, 1, 2, 3 represent the background medium and fractures oriented perpendicular to the x, y, and z axes, respectively. $\phi_i(i=0,1,2,3)$ denotes the volume fraction of the background medium and fractures in different directions, satisfying $\Sigma_{i=0,1,2,3}\phi_i=1$; σ is the effective conductivity, σ_0 is the conductivity of the background medium, and $\sigma_i(i=1,2,3)$ represents the conductivity of the fracturing fluid within fractures oriented in different directions. $R^{(i,0)}$ is the field concentration tensor.

If all fractures are filled with the same fracturing fluid, with conductivity denoted as σ_1, then equation (1) can be modified as follows,

$$\boldsymbol{\sigma} = \sigma_0 \boldsymbol{I} + \frac{1}{\phi_0}\left(\sigma_1 \boldsymbol{I} - \boldsymbol{\sigma}\right) \bullet \left[\sum_{i=1}^{3} \phi_i \boldsymbol{R}^{(i,0)}\right] \qquad (2)$$

From equation (2), it can be seen that as long as the geometric parameters and volume fractions of the hydraulic fractures, as well as the conductivities of the background medium and fracturing fluid, are given, the effective conductivity of the fracture medium can be calculated.

NUMERICAL EXAMPLE

Model I: The conductivity of the homogeneous half-space is 0.01 S/m, and the conductivity of the fracturing fluid is 1 S/m. The vertical section of the steel casing is 1 km in length, aligned with the z-axis, while the horizontal section is 560 m in length and aligned parallel to the x-axis. Three asymmetrically distributed fracturing stages labeled 1, 2 and 3 are designed gradually from the far end of a horizontal well towards a vertical well. These stages have widths of 60 m, 70 m, and 80 m respectively. Each fracturing stage contains hydraulic fractures oriented either perpendicular to the x-axis or rotated around the coordinate axes. The parameters of hydraulic fractures for each stage are shown in Table 1. The transmitting source is parallel to the y-axis, 1 km in length, located 5 km from the wellhead, emitting at a frequency of 10 Hz with an intensity of 10 A. Measurement points are uniformly distributed within the range of -500 ≤ x ≤ 700 m and -450 ≤ y ≤ 450 m, with no measurement points within 40 m of the wellhead. The differential electric field is defined as the difference between the electric fields before and after hydraulic fracturing.

Table 1 Geometric parameters of main fractures

fracturing section	w /mm	h /m	l /m	ϕ_1 /%	β /(°)	θ /(°)
1	1.5	20	140	5	0	0/30
2	1.4	20	120	3.5	0/30	0
3	1.3	20	100	4	0/30	

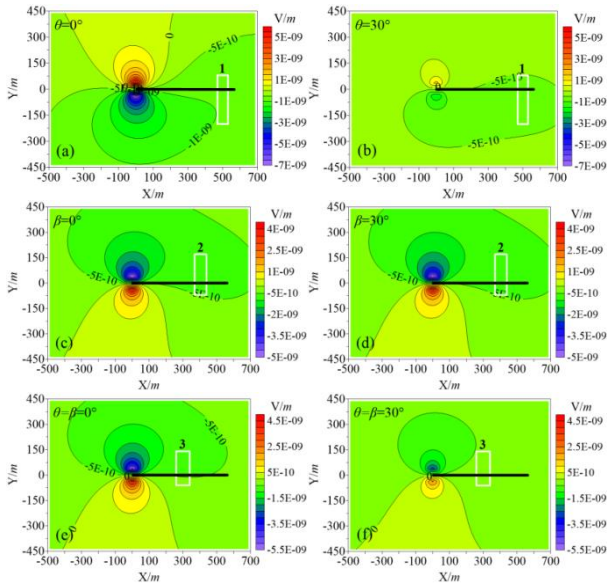

Figure 1. Contour plot of differential E_y amplitude plane (thick black line represents the projection of the horizontal well, white wireframe indicates the projection of the current fracturing stage).
(a, b) Fracturing Stage 1; (c, d) Fracturing Stage 2; (e, f) Fracturing Stage 3.

From the figure, it is evident that the distribution and rotation angle of hydraulic fractures, as well as the presence of steel casings, significantly influence the distribution of the electric field. Steel casings possess strong conductivity, reflecting anomalies of fracturing fluids from different underground locations near the wellhead. Even when the transmitting source is positioned at long offsets far from the field area, the differential electric field still exhibits the greatest variation near the wellhead. Its positive anomaly points towards the shorter end of asymmetrically distributed fracturing stages, while the negative anomaly points towards the longer end. These phenomena are observable in both the initial and final stages of multi-stage fracturing, highlighting the necessity of considering steel casings in hydraulic fracturing

models.

When hydraulic fractures rotate around the coordinate axes, the response of the differential electric field becomes more complex. Comparing Figure 1(b) with Figure 1(a), it is evident that the differential electric field is significantly influenced by the orientation angle of the fractures, resulting in a decrease in amplitude. This is because when hydraulic fractures rotate around the z-axis, the conductivity contrast in the y-direction between the fracturing stage and the surrounding rock decreases, and E_y primarily reflects the electrical structure in the y-direction of the model. The dip angle of the hydraulic fractures has almost no effect on the E_y component (Figure 1(c) and Figure 1(d)), as the electrical structure in the y-direction of the model remains unchanged when the fractures rotate around the y-axis. When hydraulic fractures have both orientation angles and dip angles simultaneously, the medium in the fracturing stage can be considered as an arbitrary anisotropic medium, resulting in a very complex response of the differential electric field (Figure 1(f)).

Model 2: This model is based on Model 1, with the surrounding rock set as a three-layer stratified medium. The first layer has a thickness of 975 m and a conductivity of 0.01 S/m, the second layer has a thickness of 50 m and a conductivity of 0.02 S/m, and the third layer has a conductivity of 0.01 S/m. Additionally, this model considers the presence of secondary fractures in each fracturing stage that are either perpendicular to the y-axis or rotated 30° around the z-axis. The volume fraction of the secondary fractures is about an order of magnitude smaller than that of the primary fractures. The geometric parameters of the secondary fractures and the equivalent anisotropic conductivities for each fracturing stage are shown in Table 2. All other parameters are identical to those in Model 1.

Table 2 Geometric parameters of secondary fractures

fracturing section	w /mm	h /m	l /m	ϕ_2 /%	θ /(°)
1	0.3	4	5	0.2	
2	0.25	3	4	0.15	0/30
3	0.2	2	3	0.18	

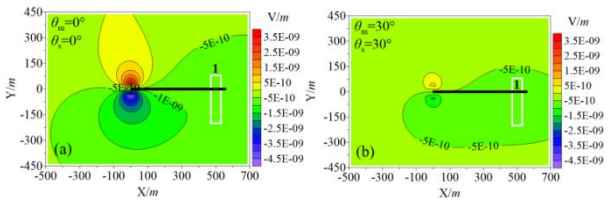

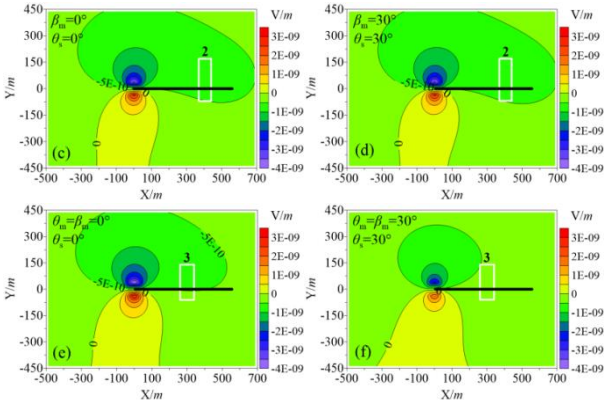

Figure 2. Contour plot of differential E_y amplitude plane for multi-stage hydraulic fracturing in a layered model(θ_m and β_m are the rotation angles of the primary fractures, θ_s is the rotation angle of the secondary fractures)
(a, b) Fracturing Stage 1; (c, d) Fracturing Stage 2; (e, f) Fracturing Stage 3

Figure 2 shows the differential results of the E_y component of the time-lapse electric field for multi-stage hydraulic fracturing in a layered model. In general, the distribution characteristics and variation patterns of the differential electric field, as well as the physical reasons causing these phenomena, are similar to the results shown in Figure 1, and will not be repeated here.

The rotation of secondary fractures around the z-axis (Figures 2(b) and 2(d)) can enhance the conductivity of the fracturing stage in the y-direction. The rotation of primary fractures around the z-axis (Figure 2(b)) or y-axis (Figure 2(d)) will weaken or not change the conductivity of the fracturing stage in the y-direction. The significantly reduced amplitude of the differential electric field in Figure 2(b) compared to Figure 2(a) and the almost identical results of Figures 2(d) and 2(c) indicate that the primary fractures play a major role in the time-lapse electric field response. In other words, the conductivity of the fracturing stage in the y-direction is mainly controlled by the primary fractures.

CONCLUSIONS

This paper establishes a relationship model between the geometric parameters of hydraulic fractures and the macroscopic equivalent conductivity using the effective medium theory. In forward calculations, this approach replaces the fracture medium in the hydrofracturing stages with a macroscopic equivalent electrical medium that can describe the micro-geometric structure of fractures. Compared to traditional methods, this approach has the following two advantages: First, it significantly improves the computational efficiency of multi-scale hydrofracturing models, allowing for

the quantitative consideration of the micro-geometric structure of fractures in forward calculations, thereby meeting industrial application requirements for computational efficiency and accuracy. Second, using the quantitative relationship established between the geometric parameters of fractures and the macroscopic anisotropic conductivity, the conductivity of the fracturing stages obtained from inversion can be converted into geometric parameters of fractures, or fracture parameters can be directly inverted from monitoring data.

Model calculations have shown that even under long-offset excitation, the primary anomalous response of the differential electric field before and after fracturing remains near the wellhead of the steel casing, independent of the horizontal position of fracturing. Under the same conditions of volume modification and injection fluid quantity, certain rotation angles of hydraulic fractures can significantly impact the time-lapse differential electric field data at the ground surface, especially with sensitivity to the fracture orientation angle. When only the dip angle is present, the distribution and amplitude of the time-lapse electric field remain nearly unchanged. Secondary fractures have a discernible influence on the ground electric field, but the primary fractures still dominate the responses.

ACKNOWLEDGEMENTS

This research is financially supported by the National Natural Science Foundation of China (42274087, 42174083) and Open Fund for Key Laboratory of Exploration Technologies for Oil and Gas Resources of MOE (K2023-08).

REFERENCES

Berryman JG, Hoversten GM (2013) Modelling electrical conductivity for earth media with macroscopic fluid-filled fractures. Geophysical Prospecting, 61(2): 471-493. doi:10.1111/j.1365-2478.2012.01135.x

Hoversten GM, Schwarzbach C. (2021) Monitoring hydraulic fracture volume using borehole to surface electromagnetic and conductive proppant. Geophysics, 86(1):E93-E109. doi:10.1190/geo2020-0410.1

Li DQ, Li F, Zhang QX, et al. (2023) Identification of fracture in electromagnetic monitoring based on improved marine predators algorithm. Progress in Geophysics (in Chinese), 38(2):677-689. doi:10.6038/pg2023GG0304

Weiss CJ, Aldridge DF, Knox HA, et al. (2016) The direct-current response of electrically conducting fractures excited by a grounded current source. Geophysics, 81(3): E201-E210. doi:10.1190/geo2015-0262.1